SIRM 2019 – 13th International Conference on Dynamics of Rotating Machines,
Copenhagen, Denmark, 13th – 15th February 2019

Application of MADYN 2000 to rotor dynamic problems of industrial machinery

Joachim Schmied [1]

[1] DELTA JS, CH-8005, Zurich, Switzerland, jschmied@delta-js.ch

Abstract

The special requirements of rotor dynamics engineering are illustrated by means of different examples of turbomachines. The properties of magnetic bearings and the more common fluid film bearings are pointed out in the examples of two turbo compressors. The importance of the correct consideration of bearing support properties is shown for a turbine generator train. The impact of seal forces is demonstrated for the turbo compressor supported on fluid film bearings. Two of the considered seals are honeycomb seals. Bearings and seals can have frequency and speed dependent characteristics; complex supports have non-negligible couplings between bearings and are frequency dependent as well. The consequences of the coupling of lateral and torsional vibrations in gears are illustrated for a gear compressor with three pinions. All examples have a practical background from troubleshooting and engineering work, although they do not exactly correspond to real cases.

Nomenclature

B	Width of bearings
d	Damping coefficient of bearings or seals
D	Diameter of bearings
	Damping ratio
f	Frequency
k	Stiffness coefficient of bearings or seals
m	Pad preload of fluid film bearings

1 Introduction

Rotors are structures with special properties due to their rotation (causing e.g. the gyroscopic effect), due to their bearings (fluid film bearings, magnetic bearings) and in many cases due to surrounding fluids (seal forces). Therefore, rotor dynamics requires special engineering tools although the structural properties of the rotors and their supports could well be modeled by any general finite element program.

Tools for rotor dynamics and bearings have been developed for many years. Nordmann, Nelson and Gasch introduced the finite element method to rotor dynamics (see [1] to [4]). Glienicke and Lund developed the basics for fluid film bearings (see [5] and [6]), which were further refined by many researchers.

The recent development of magnetic bearings, which are now more and more introduced in industrial applications of turbomachines, required an extension of existing rotordynamic tools to model the specific characteristics of this bearing type and the controllers. Spirig et al. [7] give insight into the control design process for three practical examples. This process has been further developed in the meantime and standards for design goals have been created as explained by Schmied et al. [8].

The bearing properties and resulting rotor dynamic behaviors for support on classical tilting pad fluid film bearings and magnetic bearings are illustrated for two turbo compressor examples.

The impact of the dynamics of a casing as bearing support is shown for the example of a turbine generator train with fluid film bearings.

The interaction of fluid forces in seals with rotors has been investigated by Nordmann [9] and Childs [10] to name two of the most well-known researchers in this area. A few years ago, fluid forces were mainly modeled as stiffness and damping coefficients. Recently it is more and more recognized thanks to more sophisticated analysis tools and measurements, that this approach is too restrictive. Honeycomb seals for example can have more complex

frequency dependent characteristics as shown by Kleynhans et al. [11]. Still, the rotor dynamic tools for the consideration of fluid forces are not as established as for fluid film bearings and strongly simplified engineering approaches are frequently used, for example the procedure described in the standard by the American Petroleum Institution [12] as stability level I analysis. In this paper an approach is described for a high-pressure turbo compressor, which could be used as stability level II analysis.

In train arrangements with gears the lateral and torsional vibrations are coupled. The influence of this coupling, which is not considered in standard analyses, is shown for a gear compressor.

All analyses in this paper were carried out with the general rotor dynamic program MADYN 2000. Its capabilities are described in detail by Schmied in [13]. The fluid film bearing module in MADYN 2000 is based on more than 30 years research in the German consortium FVV (Forschungsvereinigung Verbrennungskraftmaschinen / Research Association for Combustion Engines). Fuchs [14] comprehensively describes the status at the beginning of the century, which has been further developed, but basically is still valid today. The magnetic bearing module has been developed over several years based on practical needs starting with the industrial applications of magnetic bearings in turbo compressors. The developers of the module were involved from the very beginning of this area. Early applications are described by Schmied and Nijhuis et al. in [15] and [16].

2 Description of the examples

Four rotor arrangements are considered in this paper, which are described in the following chapters.

The rotor structures are modeled with finite elements according to the Timoshenko beam theory considering the shear deformation and gyroscopic effects as described by Nordmann [1], Nelson et al. [2], Gasch [4], Lund et al. [6] and Krämer [17]. Each cross section can consist of superimposed cross sections with different mass and stiffness diameter as well as different material properties. The contours shown in the rotor plot represent the resulting mass diameter with the density of the basis cross section, which is normally steel.

Stiff shrunk parts on the rotor, e.g. impellers, can be modeled as rigid parts. They are represented by mass, equatorial and polar moments of inertia. In the rotor plots they are drawn as equivalent disks. In case only the mass is given and no moments of inertias they are drawn as spheres. These parts can be fixed rigidly to the shaft, or if necessary, flexibly for example to consider disk or blade vibration modes. To model a blade mode, it may be necessary to split the mass into a rigidly mounted mass and a flexibly mounted mass representing the effective modal mass.

Several analytical results of the examples will be shown: Campbell diagrams, i.e. damped natural vibration modes at different speeds, and the response to unbalance loads. The damping in the Campbell diagrams is described as damping ratio, which can easily be transformed to an amplification factor in resonance. The damping from the Campbell diagram is unequivocal and accurate in contrast to the damping from an unbalance response received by the half power width method, as it is described in for example in the standard American Petroleum Institution [12]. The stability can also be assessed by the damping ratio; an unstable rotor has a negative damping ratio.

2.1 Turbo compressor supported on fluid film bearings with seals

The model of the turbo compressor is shown in figure 1. Its maximum speed is 12’000 rpm and the total rotor weight 220 kg. This example will also be used to demonstrate the impact of seal fluid forces. The location of the two considered labyrinth seals and honeycomb seals with the highest gas density are shown in the figure.

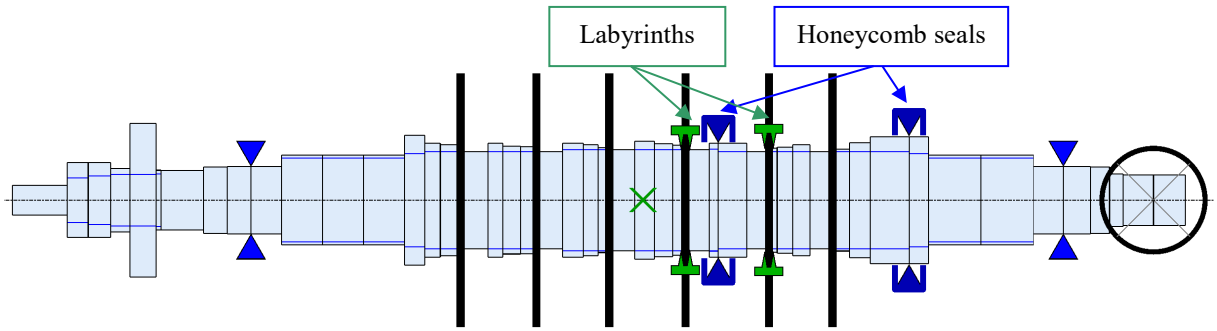

Figure 1: Compressor rotor on fluid film bearings with seals.

The geometry of the 4 tilting pad bearings is illustrated in figure 2. The bearing has a load between pads arrangement. The pads have a central support.

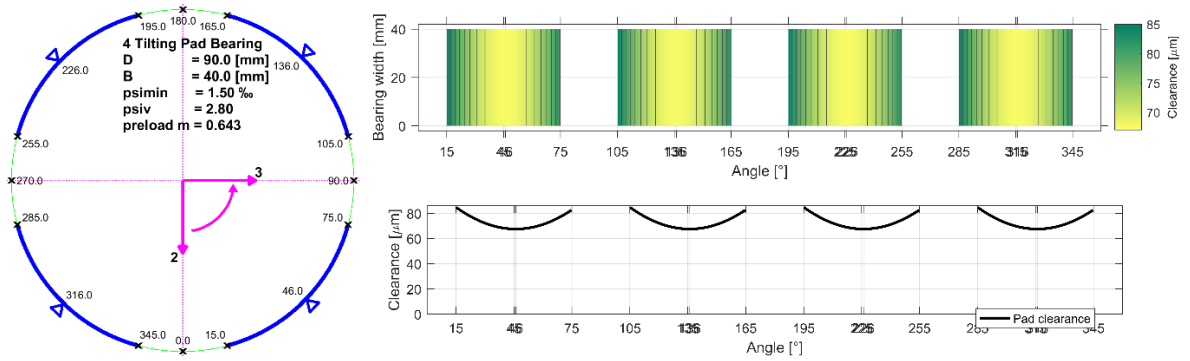

Figure 2: Radial fluid film bearing geometry and clearance plot.

2.2 Turbo compressor on magnetic bearings

The model of the turbo compressor is shown in figure 3. Its maximum speed is 12'600 rpm and the total rotor weight 550 kg. The bearings are represented by their sensor and actuator. The triangle in the plot indicates the actuator location, the bar the sensor location.

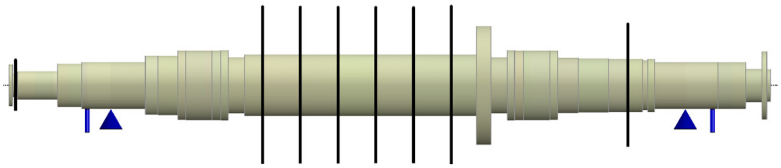

Figure 3: Turbo compressor on magnetic bearings.

2.3 Turbine generator train

The model of the turbine generator train is shown in figure 4. Its nominal speed is 3'000rpm. Turbine and generator are supported on fixed pad fluid film bearings.

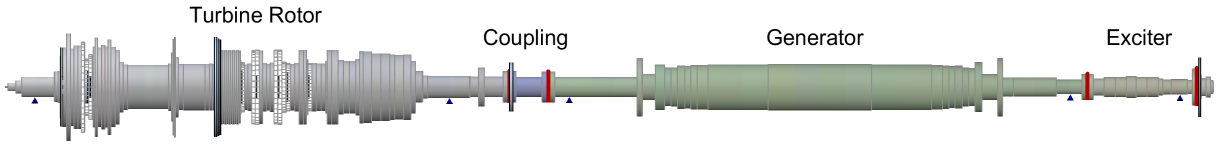

Figure 4: Turbine generator shaft train.

The turbine rotor casing is considered as a state space model, which is gained from the natural modes of a finite element model of the casing. The method is described by Krüger in [18]. In the present case ANSYS was used to receive the state space matrices in a so called spm-file, which can directly be imported to MADYN 2000 as explained by Schmied in [19]. When importing the state space matrices to MADYN 2000 a structural damping can be defined, in our example it is 1%. The ANSYS system does not have any damping. The amplitudes of the transfer functions of the coupled turbine casing can be seen in figure 5.

Each column in figure 5 corresponds to the location/direction of an excitation and each row to the location/direction of the response. Locations are the turbine NDE (left, STA 4) and DE (right STA 100) bearings and directions are 2 (vertical) and 3 (horizontal). The couplings of the casing between the two bearings are rather strong, i.e. their amplitude has the same order of magnitude as the amplitude of the direct transfer functions on the diagonal, whereas the couplings between the directions is weak.

The generator and exciter have simple spring, mass supports. Each support has a resonance in horizontal and vertical direction in the range of three times operating speed. Such support models are used in traditional rotor dynamic analyses. In case a support has only one relevant resonance in each direction and the coupling between supports is negligible, such a model is sufficient.

For the turbine such a support model was also used originally. It proved to be insufficient as we will see later in this paper.

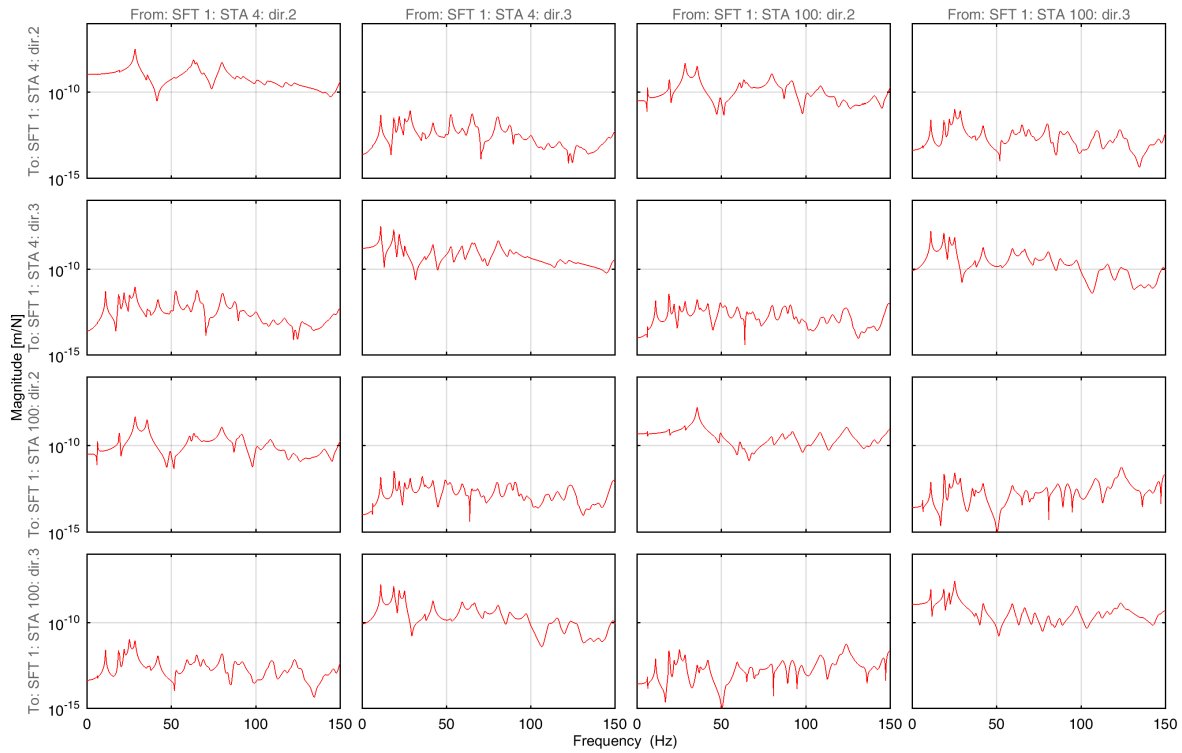

Figure 5: Transfer functions of the turbine casing.

In a shaft train consisting of two rotors with two bearings each and coupled with a solid coupling the static bearing load and thus the bearing characteristics depend on the alignment, which may change due to thermal growths of supports and casings. MADYN 2000 allows static analyses for different alignments and finding an optimal alignment for minimum forces in the coupling flanges. In this example the influence of different alignments is relatively small due to the high weight of the rotors and the flexibility of the solid coupling.

2.4 Gear compressor

The model of the gear compressor consisting of a bull gear and three pinions is shown in figure 7. All rotors are supported on fluid film bearings, the pinions on tilting pad bearings and the bull gear on cylindrical bearings. The meshing is modelled as explained in the figure next to the model plot. The spring is aligned with the tooth contact force. Its direction is indicated by the magenta line.

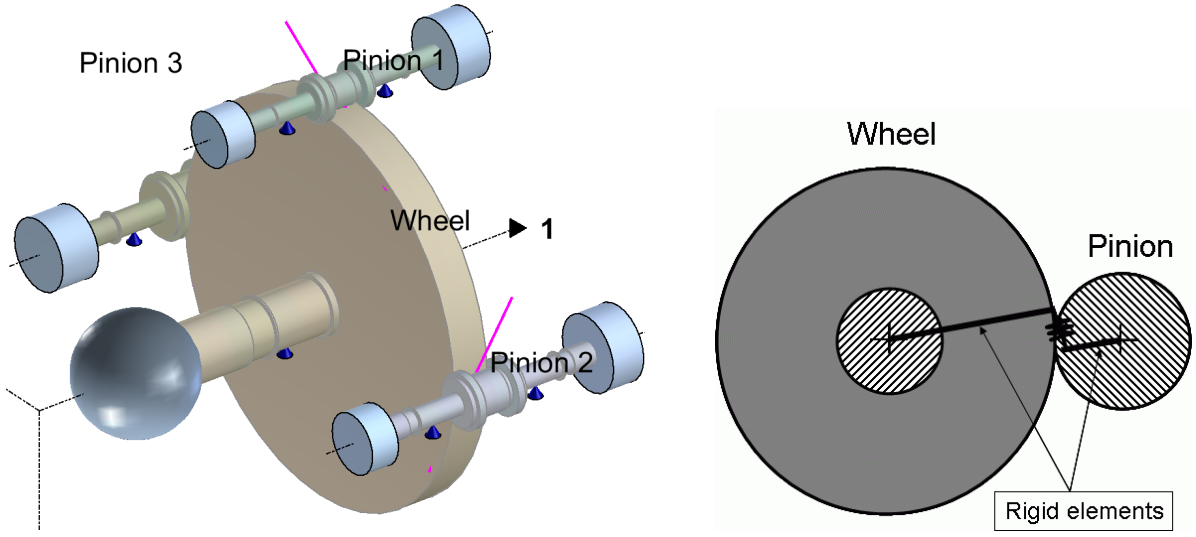

Figure 6: Gear compressor with explanation of the gear mesh model.

3 Rotor dynamic behaviour with fluid film bearings and magnetic bearings

3.1 Rotor on fluid film bearings

The stiffness and damping coefficients of the fluid film bearings in the 2-3 coordinate system of figure 2 are shown in figure 7 together with the static position in the bearing at different speed (Gümbel curve). Due to the pad arrangement the bearing is isentropic, i.e. the coefficients in 2- and 3-direction are equal. Moreover, there are no cross-coupling terms. The coefficients of the two bearings are almost the same. For this reason, the results of only one bearing is shown.

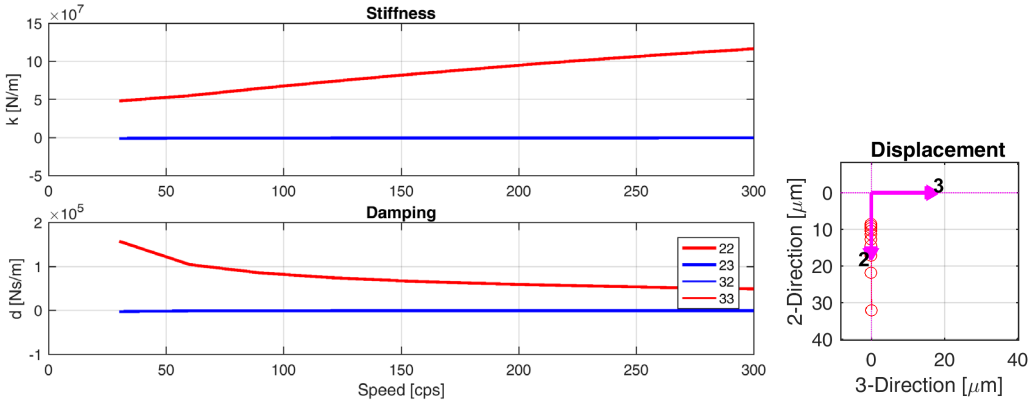

Figure 7: Stiffness and damping coefficients of the fluid film bearing with Gümbel curve.

The coefficients of fluid film bearings are load dependent (the load in the present case is the rotor weight) and speed dependent. However, for tilting pad bearings they can additionally be frequency dependent, i.e. the stiffness and damping at a certain speed for vibrations with non-synchronous frequencies is different. This effect can be considered by a full model of the tilting pad bearing, i.e. keeping the tilting angles in the bearing model and not reducing them, what is normally done under the assumption, that tangential pad forces are negligible. A full model can be represented in state space form with the rotor displacement and velocities as inputs, the radial forces as outputs and the pad tilting angles and their derivatives in time as states. More details are described by Schmied et al. [20]. The non-synchronous coefficients of the same bearing at the nominal speed of 210 rps are shown in figure 8. The synchronous coefficients are highlighted with data tips. They correspond to the coefficient in figure 7 at 210 cps. For lower frequencies at this speed the stiffness increases and the damping decreases. These trends tend to reduce the damping of modes in the sub-synchronous frequency range.

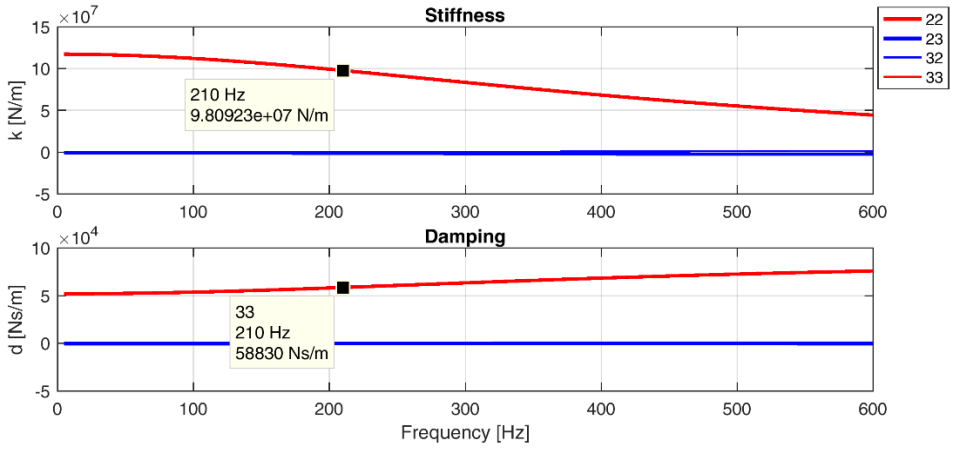

Figure 8: Non-synchronous stiffness and damping coefficients at nominal speed of 210 rps.

The Campbell diagram (natural frequencies and damping ratios as a function of speed) calculated with the full model i.e. correct non-synchronous characteristics is shown in figure 9. The dashed line for the damping is for mode 2 calculated with bearing coefficients neglecting the frequency dependence, i.e. in the traditional way. It can be seen, that the damping with the correct non-synchronous characteristics is indeed lower at nominal speed, as expected from the trends in figure 8. The damping reduces from 10.6% to 8.2%.

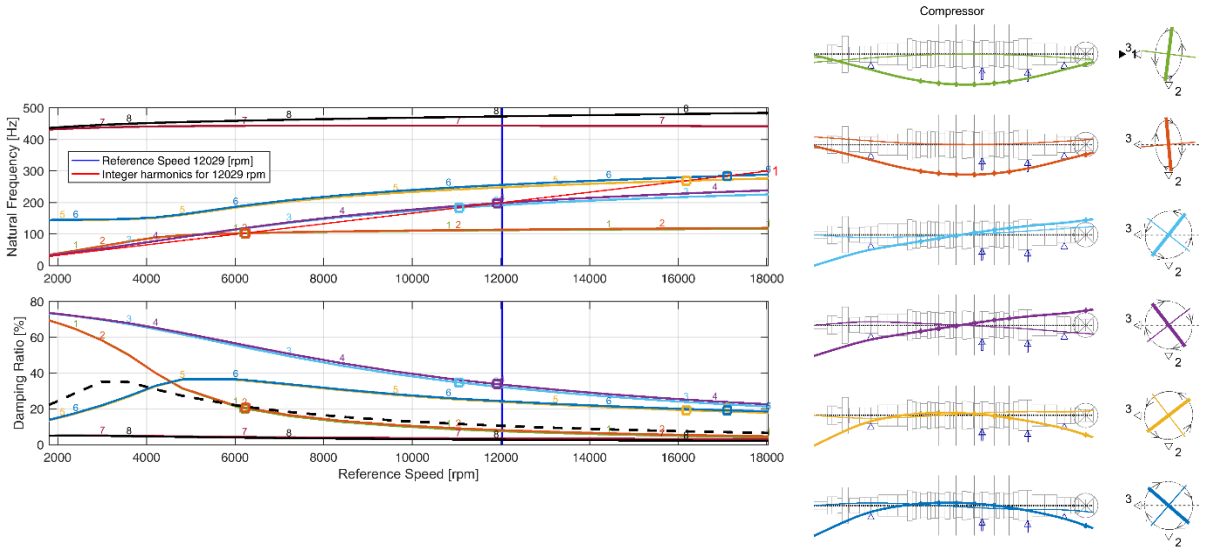

Figure 9: Campbell diagram (dashed line damping mode 2 with syn. coeff.) and mode shapes in critical speeds

The mode shapes in critical speeds can also be seen in figure 9 in compact form. MADYN 2000 has another 3-dimensional presentation of modes. In the compact form they are shown in two planes at the instant when the maximum deflection occurs. The first plane is determined by the maximum deflection and the rotor axis and the second plane is perpendicular to this plane. The first plane is indicated by the bold line in the 2-3 coordinate system and the second plane by the thin line. The whirling direction is also indicated in the figure. A circular forward whirling orbit has the value +1 and a circular backward whirling mode the value -1. Elliptic orbits have values between 0 and +1 and -1 respectively.

The rotor runs clearly above its first bending. The tilting mode is very close to the nominal speed. It has a large damping ratio of more than 30%, thus this resonance is not a problem. Standards such as API allow running in a resonance, if the damping is above 20% corresponding to an amplification factor smaller than 2.5.

3.2 Rotor on magnetic bearings

In figure 10 the bearing characteristics of the magnetic bearings are shown as transfer functions describing the relation between the rotor displacement at the sensor and the actuator force. The characteristics are highly frequency dependent. However, they do not change with speed. The hardware consisting of sensor, amplifier and actuator, the controller and digitization effects are included in the transfer functions. The hardware causes a continuous phase lag with increasing frequency, i.e. a reduction of damping. The ranges with bold lines indicate where the bearings have a damping characteristic (phase angles between 0 and 90 degree or below -180 degree). The eigenvalues (natural frequency and damping ratio) of the complete system (bearing and rotor) at maximum speed are also shown in figure 10. The transfer functions are determined to a large extent by the controllers. The design of a controller requires extensive engineering effort. It is described for example by Schmied et al. [8]. Goals of the design are to receive a robust, stable system with enough damping in the speed range. Robustness must be fulfilled against system changes (the model deviates to some extent of the real system) and against noise in the magnetic bearing system, which requires the gain to remain below a certain level.

The mode shapes in two perpendicular planes as described for figure 9 are shown in figure 11. The shapes move on circles, because the bearings are completely isotropic.

It can be seen, that all modes below maximum speed are well damped and that all modes in the higher frequency range are stable. Some modes are not determined by the rotor but by the controller, which augments the system and causes additional modes.

Compared to the rotor on fluid film bearings the behaviour is quite different. There are two pairs of forward and backward whirling well damped rigid body modes at low frequencies. They appear due to low bearing stiffness in this frequency range, which can be recognized in the transfer function in figure 10. The transfer function has a value well below 10^8 N/m. This is lower than the stiffness of the fluid film bearing of the other rotor, despite the fact, that the rotor for fluid film bearings is considerable smaller. The first bending modes occur at 155Hz and 162Hz, respectively. Their shape corresponds more to a free - free bending mode shape. In the present case this mode is within the speed range and the damping of more than 20% allows running in resonance.

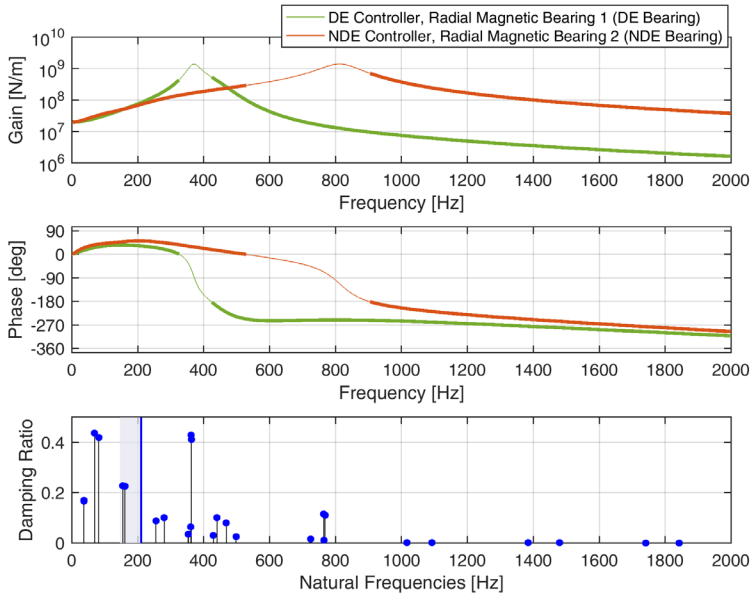

Figure 10: Magnetic bearing transfer functions and eigenvalues (damping and natural frequencies)

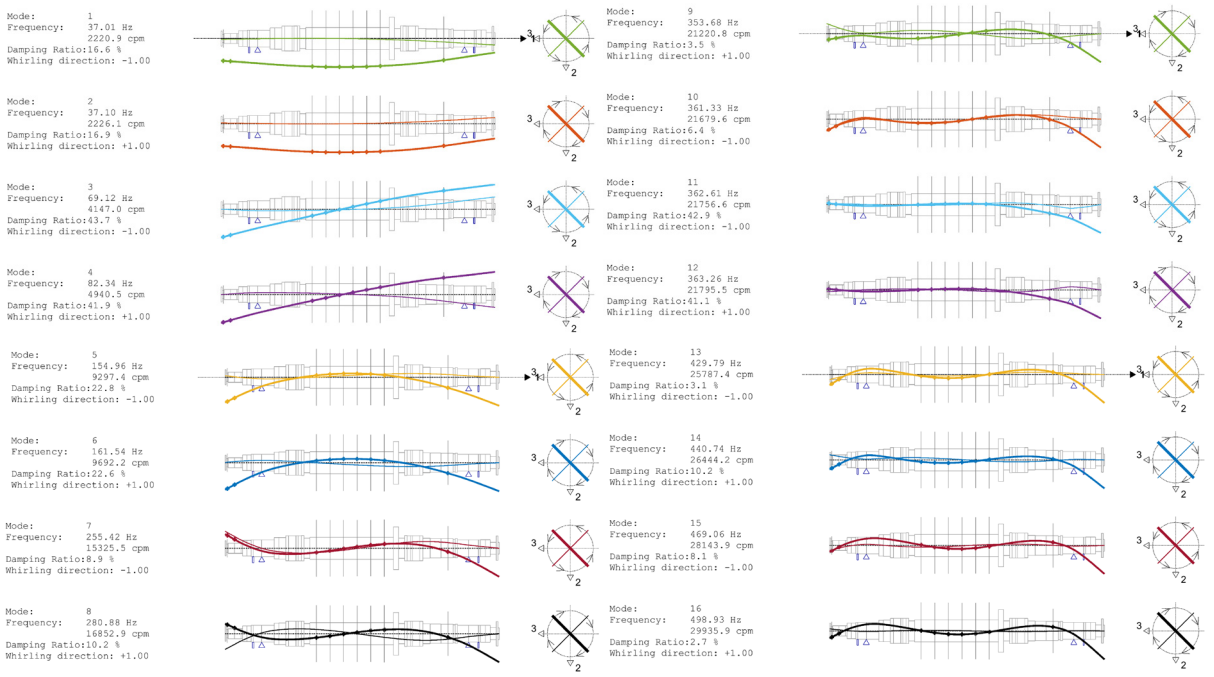

Figure 11: Natural modes nominal speed.

4. The influence of bearing supports

The Campbell diagram of the turbine generator shaft train including the turbine casing and the spring mass supports for the generator and exciter bearings is shown in figure 12. The number of modes is huge, because the system has many turbine casing modes. Some of the turbine modes couple with the rotor, some not. In figure 12 two examples of modes in critical speeds are shown: one mode which is mainly a casing mode, and another coupled rotor casing mode. The casing mode has no relative displacement between rotor and casing displacement in contrast to the coupled mode. Casing modes are also characterized by their damping of 1%, which is the structural casing damping. Casing modes, which couple with the rotor, have a different damping; normally it is higher, because some of the bearing damping is transferred.

The Campbell diagram of a coupled rotor casing systems can be complex. Unbalance response analyses are a big help to find the relevance of modes and their resonances. Some of the casing modes for example may be difficult to excite, due to their shape or due to their big effective mass. The relative vibrations at the turbine bearings of a response to an unbalance are shown in figure 13 for the model with the complex casing characteristics and a

model with simple bearing support. A comparison of the two responses reveals the importance of a correct casing model. The resonances are completely different. The traditionally still widely used simple supports are not always suitable.

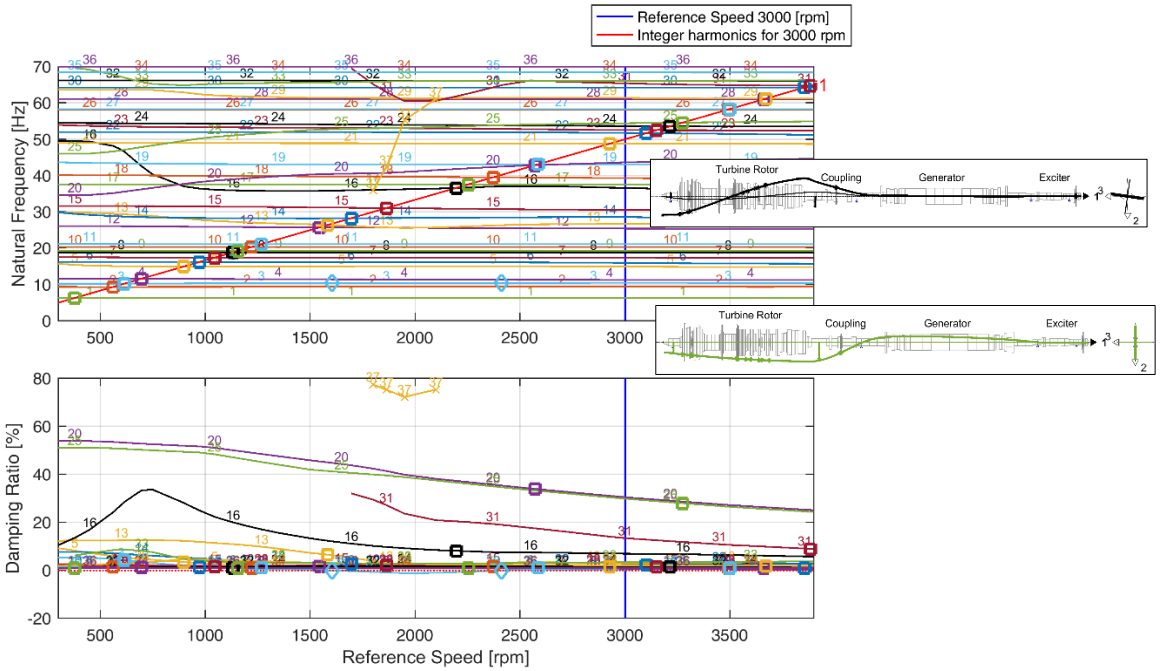

Figure 12: Campbell diagram with two exemplary critical mode shapes (dominated by casing and coupled).

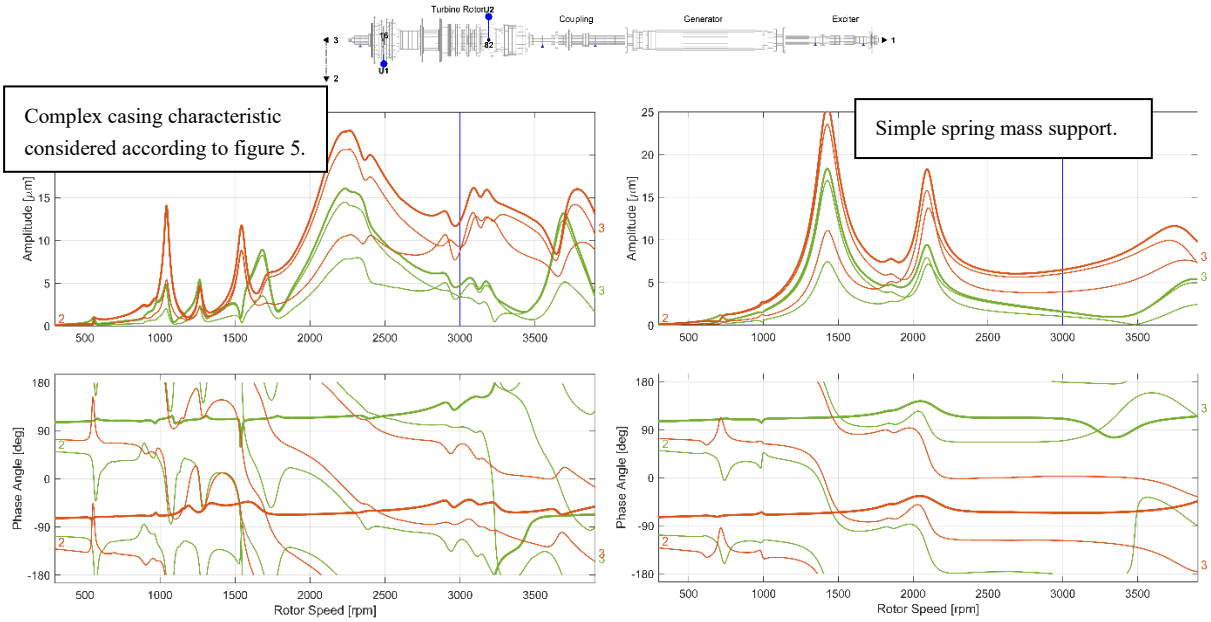

Figure 13: Unbalance load and response (relative vibrations at turbine bearings).

5. The impact of seal forces

The tangential and radial seal forces of the labyrinths of the rotor in figure 3 for a circular unit shaft orbit are shown in figure 14. They are the forces from the seal on the rotor, i.e. positive tangential forces destabilize forward whirling modes and positive radial forces are in the same direction as the orbit radius, i.e. they bring the rotor out of centre and thus soften the system.

The labyrinth seal forces were calculated with a Navier Stokes solver described by Weiser in [21]. The tangential as well as radial force show a slight curvature caused by inertia effects. To include them in the model, mass coefficients are necessary. In the present case the inertia effect is small.

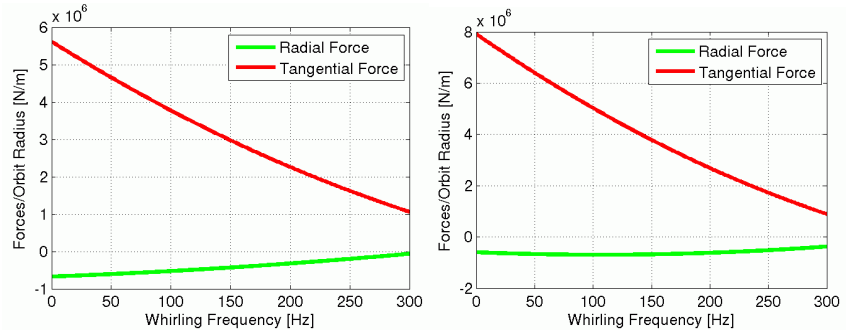

Figure 14: Radial and tangential labyrinth seal forces

The frequency at which the tangential force is zero, the so-called swirl frequency, allows a rough assessment, which rotor modes are destabilized by the seals: Forward whirling modes with lower frequencies will be subjected to a damping reduction. For the labyrinth seals this frequency is beyond the shown frequency range to 300Hz.

The honeycomb seal forces in figure 15 for circular backward (neg. frequency) and forward (pos. frequency) orbits are strongly frequency dependent. They were calculated according to the method described by Kleynhans in [11] and cannot be simply modelled by stiffness, damping and mass coefficients. They must be modelled by transfer functions in a similar way as magnetic bearings.

The swirl frequencies of the balance piston and interstage seal are around 50Hz and 70Hz, respectively.

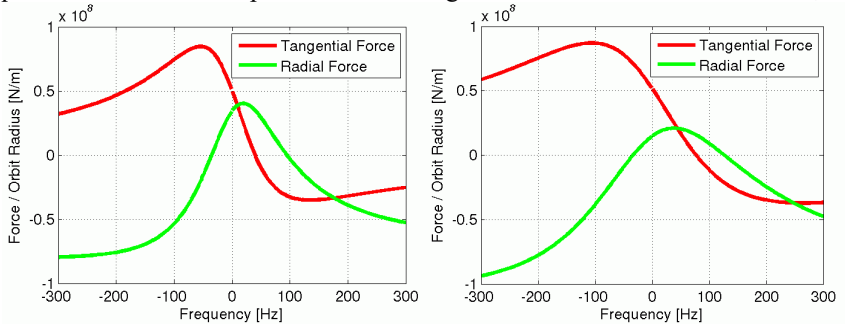

Figure 15: Radial and tangential honeycomb seal forces

The eigenvalues of the system with and without the seals are shown in figure 16. The seals are considered in two steps for a better interpretation of the results. In a first step only the labyrinth seals are considered and in a second step all seals.

The labyrinth seals mainly influence the forward and backward whirling first bending mode. The damping of the forward mode is decreased, of the backward mode increased. The other modes are almost not affected.

The impact of the honeycomb labyrinth seals is very big in a frequency range up to 250Hz. The system with honeycomb seals is well damped. This is due to the large stiffening effect at higher frequencies (negative radial force) and the relatively low swirl frequency.

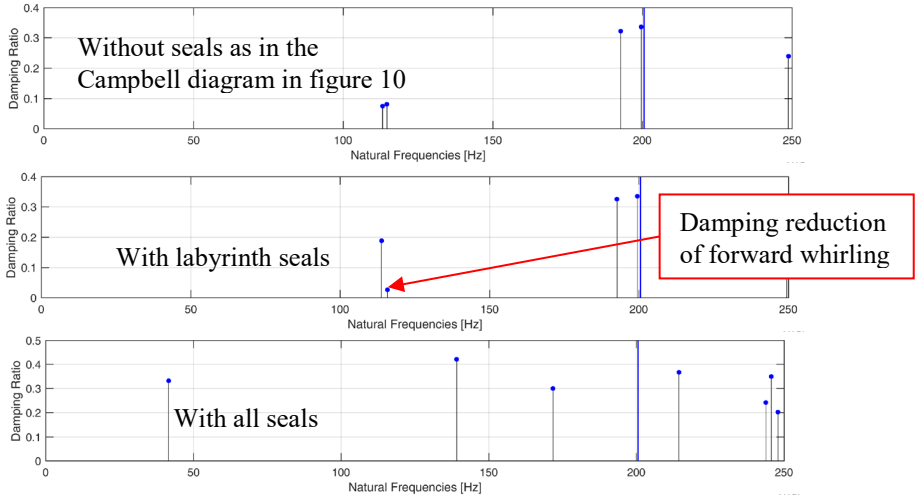

Figure 16: Eigenvalues at nominal speed without and with consideration of seal forces

6. Coupling of torsional and lateral vibrations in gears

The coupling of lateral and torsional vibrations in gears is normally not considered. An additional coupling with axial vibrations can also occur. Lateral torsional coupling is of interest for the following reasons:

Due to the lateral vibration component the radial bearings can influence the damping of the torsional vibration modes. Normally they add damping, but they can also destabilize as reported for example by Viggiano et al. in [22]. This reference also contains a comparison of measured and calculated stability thresholds, verifying this type of analysis.

Lateral excitations such as the unbalance can excite torsional vibrations and vice versa torsional excitations excite lateral vibrations. By means of a coupled model this can be simulated.

The natural vibration modes of a lateral torsional coupled model can be different from those of the decoupled systems. For our example this is shown in figure 17, where a selection of modes of the standalone pinion 1 are shown together with modes of the coupled system, which are dominated by this pinion.

Some modes practically do not change due to the coupling as the mode at 118 Hz. On the other side completely new modes can appear as the mode at 173 Hz and modes can couple as the torsional mode at 345 Hz and the lateral mode at 419 Hz of the pinion, which are combined to a coupled lateral torsional mode at 360 Hz.

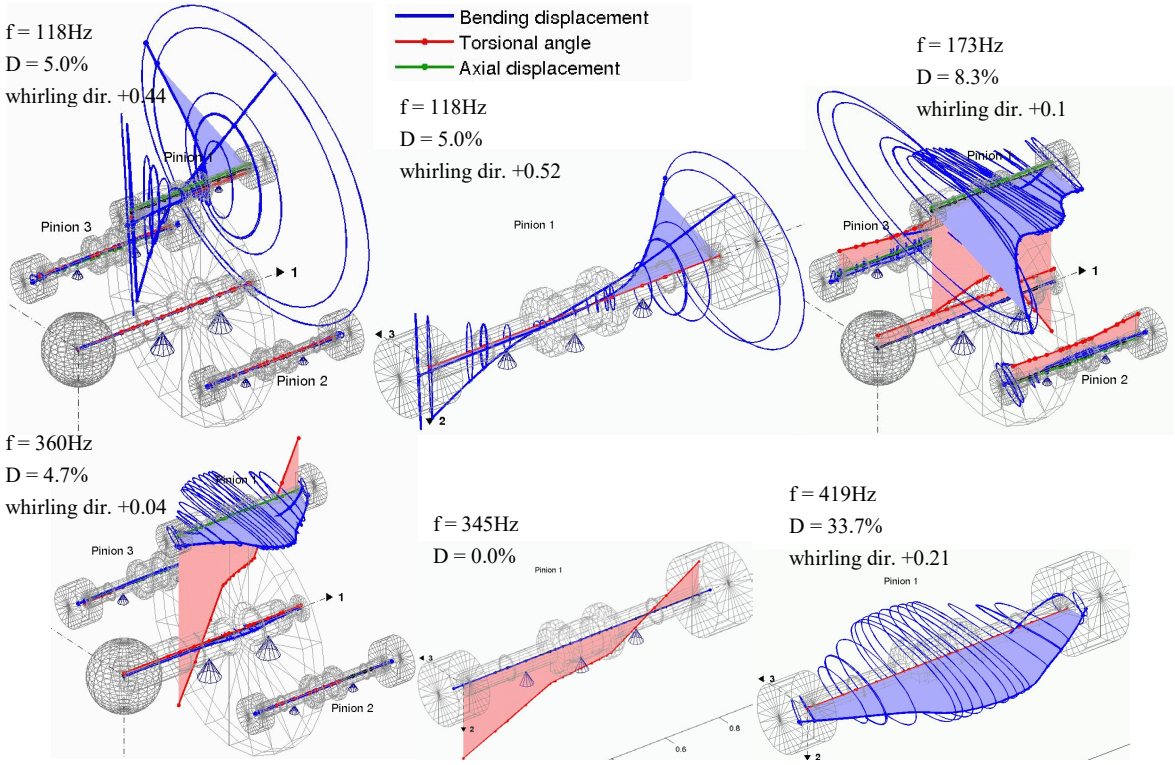

Figure 17: Lateral and torsional modes of pinion 1 of the coupled and uncoupled system

7 Conclusion

The requirements of a modern tool for rotor dynamic analyses are demonstrated for four examples, covering different types of bearings, the influence of casing dynamics, seal forces acting on rotors and coupled vibrations as they can occur in gears.

Some of the requirements are new due to new bearing technologies (e.g. magnetic bearings) or new research results (e.g. the frequency dependence of seal forces and tilting pad bearings). In both cases the forces caused by rotor displacements are strongly frequency dependent and cannot be simply modelled by stiffness, damping and mass coefficients.

To cover these needs MADYN 2000 uses state space representation for frequency dependent bearings. State space matrices are also used for the import of complex support structures. For support structures the input to the system are forces and the outputs displacements and velocities, whereas for the bearings the inputs are displacements and velocities and the outputs forces.

References

[1] Rainer Nordmann (1974). *Ein Näherungsverfahren zur Berechnung der Eigenwerte und Eigenformen von Turborotoren mit Gleitlagern, Spalterregung, äusserer und innerer Dämpfung.* Dissertation Technische Hochschule Darmstadt.

[2] H.D. Nelson, J.M. McVaugh (1976). The Dynamics of Rotor-Bearing Systems using Finite Element. *ASME Trans., Journal of Industry*, Vol. 98(2), pp.593-600.

[3] H.D. Nelson (1980). A Finite Rotating Shaft Element using Timoshenko Beam Theory. *Trans. ASME, Journal of Mechanical Design*, Vol. 102(4), pp.793-803.

[4] Rainer Gasch (1976). Vibration of Large Turbo-Rotors in Fluid Film Bearings on an Elastic Foundation. *Journal of Sound and Vibration*, Vol. 120, pp.175-182.

[5] Joachim Glienicke (1966). *Feder- und Dämpfungskonstanten von Gleitlagern für Turbomaschinen und deren Einfluss auf das Schwingungsverhalten eines einfachen Rotors.* Dissertation Technische Hochschule Karlsruhe.

[6] J. Lund, K. Thomsen (1978). A Calculation Method and Data for the Dynamics of Oil Lubricated Journal Bearings in Fluid Film Bearings and Rotor Bearings System Design and Optimization. *ASME*, New York (1978), pp. 1-28.

[7] M. Spirig, J. Schmied, P. Jenckel, U. Kanne (2002). Three Practical Examples of Magnetic Bearing Control Design Using a Modern Tool. *ASME Journal of Engineering for Gas Turbines and Power*, October 2002, Vol. 124, pp. 1025-1031.

[8] J. Schmied, A. Kosenkov (2013). Practical Control Design for Rotor on Magnetic Bearings by Means of an Efficient Tool. *Proceedings of ASME Turbo Expo*, San Antonio, Texas, USA.

[9] R. Nordmann, F.J. Dietzen (1987). Calculating Rotordynamic Coefficients of Seals by Finite-Difference Techniques. *ASME Journal of Tribology*, July 1987, Vol. 109, pp. 388-394.

[10] Dara Childs (1993). *Turbomachinery Rotordynamics*. Wiley Inter Science Publication, New York, Chichester, Brisbane, Toronto, Singapore.

[11] G.F. Kleynhans, D. Childs, (1996). The Acoustic Influence of Cell Depth on the Rotordynamic Characteristics of Smooth Rotor / Honeycomb-Stator Annular Gas Seals. *ASME* paper No. 96-GT-122, presented at the ASME Turbo Expo, Birmingham, UK, 1996.

[12] American Petroleum Institution (2002). Axial and Centrifugal Compressors and Expander-compressors for Petroleum, Chemical and Gas Industry. *API Standard 617*, 7th edition.

[13] Joachim Schmied (2017). *MADYN 2000 Documentation Version 4.4*. Internal document DELTA JS, Zurich, Switzerland.

[14] Andreas Fuchs (2002). *Schnellaufende Radialgleitlagerungen im instationären Betrieb.* Dissertation Technische Universität Braunschweig.

[15] Joachim Schmied (1990). Experience with Magnetic Bearings Supporting a Pipeline Compressor. *Proceedings 2nd Symposium on Magnetic Bearings*, Tokyo, Japan.

[16] A.B.M. Nijhuis, J. Schmied, R.R. Schultz (1999). Rotordynamic Design Considerations for a 23MW Compressor with Magnetic Bearings. *IMechE Fluid Machinery Symposium*, The Hague, Netherlands.

[17] Erwin Krämer (1984). *Maschinendynamik.* Springer Verlag, Berlin, Heidelberg, New York, Tokyo.

[18] Thomas Krüger, Sauro Liberatore, Eric Knopf (2013). Complex Substructures And Their Impact On Rotordynamics. *Proceedings of SIRM 2013 – 10th International Conference on Vibrations in Rotating Machines*, Berlin, Germany.

[19] Joachim Schmied, Marco Perucchi (2017). Coupled Rotor-Bearing-Casing Analysis. *22nd Swiss CADFEM ANSYS Simulation Conference*, Switzerland.

[20] J. Schmied, A. Fedorov, B.S. Grigoriev (2010). Non-Synchronous Tilting Pad Bearing Characteristics. *Proceedings of the 8th IFTOMM International Conference on Rotordynamics*, KIST, Seoul, Korea.

[21] H.P. Weiser (1989). *Ein Beitrag zur Berechnung dynamischer Koeffizienten von Labyrinthdichtungs-systemen bei turbulenter Durchströmung mit kompressiblen Medien.* Dissertation TU Kaiserslautern.

[22] F. Viggiano, J. Schmied (1996). Torsional Instability of a geared compressor shaft train. *IMechE* paper C508/013.